Acta Cryst E CRYSTALLOGRAPHIC COMMUNICATIONS

ISSN 2056-9890

Synthesis, crystal structure and Hirshfeld surface analysis of 1-(3,4-dichlorophenyl)-4,4,6-trimethyl-3,4-dihydropyrimidine-2(1*H*)-thione

Sharatha Kumar[a]* and Tuncer Hökelek[b]

[a]Department of Chemistry, Yenepoya Institute of Arts, Science, Commerce and Management, Mangaluru, Yenepoya University (Deemed to be University), 575013 Karnataka, India, and [b]Hacettepe University, Department of Physics, 06800 Beytepe-Ankara, Türkiye. *Correspondence e-mail: sharathyiascm@yenepoya.edu.in

Received 16 June 2026
Accepted 14 July 2026

Edited by N. Alvarez Failache, Universidad de la Repüblica, Uruguay

Keywords: pyrimidine; 3,4-dichlorophenyl; crystal structure.

CCDC reference: 1816810

Supporting information: this article has supporting information at journals.iucr.org/e

The title compound, $C_{13}H_{14}Cl_2N_2S$, consists of dichlorophenyl and dihydropyrimidinethione rings, where the pyrimidine ring is in a flattened-boat conformation. In the crystal, N—H···S hydrogen bonds link the molecules, enclosing $R_2^2(8)$ ring motifs, into centrosymmetric dimers. Neither π–π stacking nor C—H···π(ring) interactions are observed. Hirshfeld surface analysis revealed that the most important contributions for crystal packing are from H···H (40.8%), H···Cl/Cl···H (28.7%) and H···S/S···H (15.5%) interactions. The volume of the crystal voids and the percentage of free space were calculated to be 135.01 Å^3 and 17.99%, showing the crystal packing is not compact. Computational methods indicated an N—H···S hydrogen-bonding energy of −58.2 kJ mol^{-1}. Evaluations of the electrostatic, dispersion and total energy frameworks indicate that the crystal cohesion is dominated by electrostatic energy contributions.

1. Chemical context

Heterocyclic compounds containing pyrimidine and dihydropyrimidine frameworks have attracted sustained interest because of their wide range of biological and pharmacological activities, including antibacterial, antifungal, antitubercular and anti-inflammatory properties (Kappe, 2000; Leite *et al.*, 2006; Sriram *et al.*, 2006). In particular, Biginelli-type dihydropyrimidine derivatives are recognized as important structural motifs in medicinal chemistry and synthetic organic chemistry owing to their diverse therapeutic potentials and convenient synthetic accessibilities.

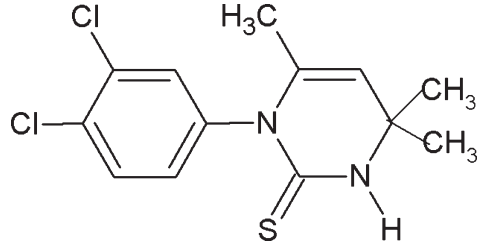

Continuing our interest in the syntheses and structural characterizations of biologically significant heterocyclic compounds (Alam *et al.*, 2005), the title compound was prepared and investigated. Herein, we report its molecular and crystal structures together with the results of Hirshfeld surface (HS), crystal void analyses and interaction energy calculations and energy frameworks of the title compound, (I).

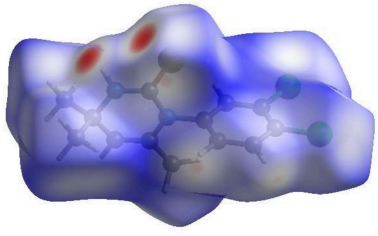

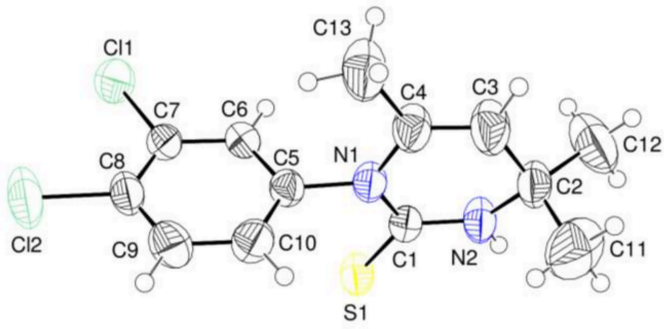

Figure 1
The asymmetric unit with the atom-numbering scheme and 50% probability ellipsoids.

Figure 2
Conformation of the pyrimidine ring.

2. Structural commentary

The title compound, (I), contains a planar phenyl ring and a six-membered nitrogen-containing heterocyclic dihydropyrimidinethione ring (Fig. 1). The 3,4-dichlorophenyl, dimethyl and methyl substituents are bonded to the 3,4-dihydropyrimidine-2(*1H*)-thione ring at the N1, C2 and C4 positions, respectively. The pyrimidine, *A* (N1/N2/C1–C4), ring is in flattened-boat conformation (Fig. 2) with puckering parameters (Cremer & Pople, 1975) Q_T = 0.184 (3) Å, θ = 70.8 (9)° and φ = 174.4 (11)°. It is reported to be planar in 4,4,6-trimethyl-1-phenyl-3,4-dihydro-pyrimidine-2(1*H*)-thione [(II); Yamin *et al.*, 2005], N-benzoyl-*N*′-phenylthiourea [(III); Yamin & Yusof, 2003] and 1-ethyl-5-(4-methoxybenzoyl)-4-(4-methoxyphenyl)pyrimidine-2(*1H*)-thione [(IV); Özçelik *et al.*, 2004]. The S1═C1 [1.692 (2) Å], C1—N1 [1.361 (3) Å] and C1—N2 [1.323 (3) Å] bond lengths are comparable with the corresponding values in compounds II—IV. Other bond lengths are in normal ranges (Allen *et al.*, 1987).

3. Supramolecular features, Hirshfeld surface analysis, void analysis, interaction energies and energy frameworks

In the crystal, N—H···S hydrogen bonds (Table 1) link the molecules, enclosing $R_2^2(8)$ ring motifs (Etter *et al.*, 1990), into centrosymmetric dimers (Fig. 3*a*). The supramolecular dimer formation through the N—H···S hydrogen bonds is shown in Fig. 3*b*. Neither π–π stacking nor C—H···π(ring) interactions are observed.

The intermolecular interactions in the crystal were visualized by carrying out a Hirshfeld surface (HS) analysis using *CrystalExplorer* 17.5 (Spackman *et al.*, 2021). Fig. 4 shows the Hirshfeld surface with several neighbouring molecules in the

Table 1
Hydrogen-bond geometry (Å, °).

D—H···*A*	*D*—H	H···*A*	*D*···*A*	*D*—H···*A*
N2—H2*N*···S1^{i}	0.85 (2)	2.55 (2)	3.375 (2)	163 (3)

Symmetry code: (i) $-x, -y+1, -z$.

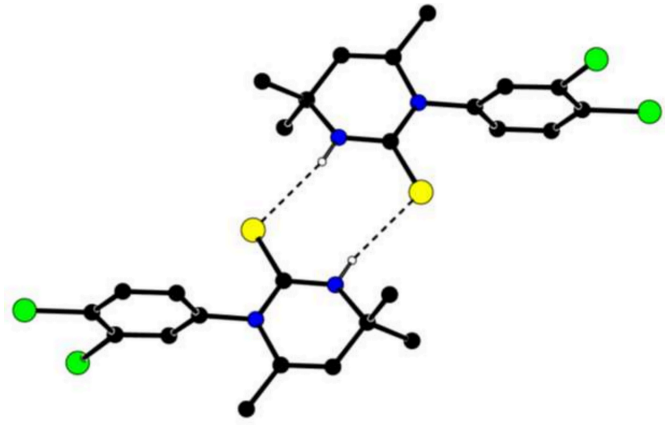

(a)

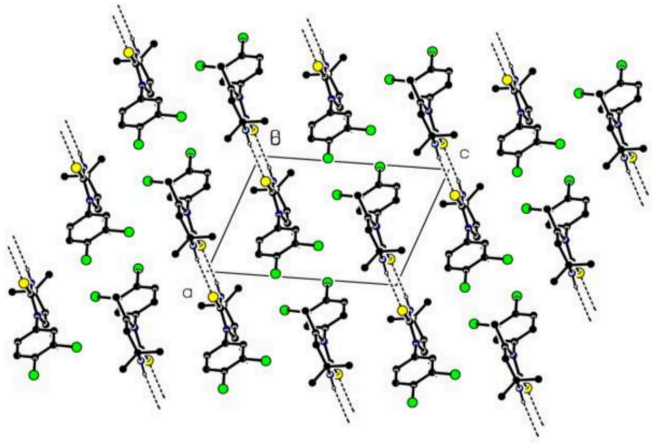

(b)

Figure 3
(*a*) The dimer formation through N—H···S hydrogen bonds (shown as dashed lines) with an $R_2^2(8)$ ring motif. (*b*) A partial packing diagram viewed down the *b*-axis direction showing the supramolecular dimer formation. The N—H···S hydrogen bonds are shown as dashed lines.

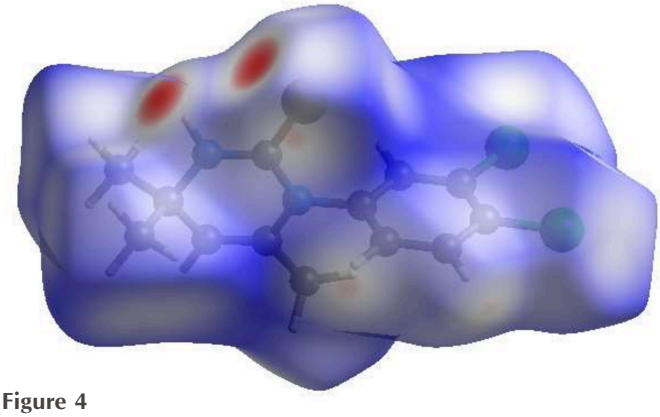

Figure 4
View of the three-dimensional Hirshfeld surface plotted over d_{norm} in the range −0.3452 to 1.4957 a.u.

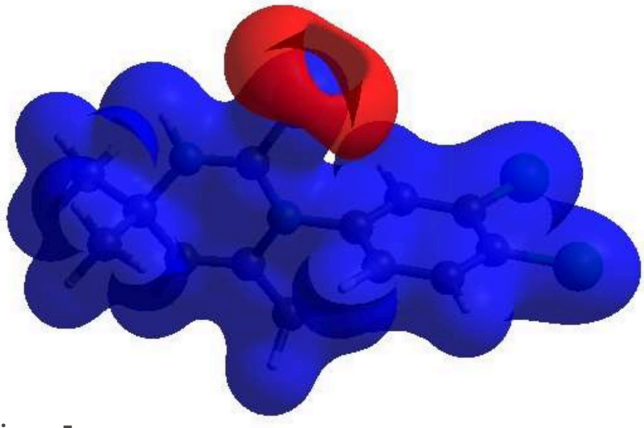

Figure 5
View of the three-dimensional Hirshfeld surface of the title compound plotted over electrostatic potential in the range −0.0500 to 0.0500 a.u. using the STO-3 G basis set at the Hartree–Fock level of theory. Hydrogen-bond donors and acceptors are shown as blue and red regions around the atoms, corresponding to positive and negative potentials, respectively.

crystal. The white surface indicates contacts with distances equal to the sum of van der Waals radii, and the red and blue colours indicate distances shorter (in close contact) or longer (distant contacts) than the sum of the van der Waals radii, respectively. The red spots indicate their roles as the respective donors and/or acceptors atoms in hydrogen bonding, as discussed above; they also appear as the blue and red regions corresponding to positive and negative potentials on the HS mapped over electrostatic potential as shown in Fig. 5. The blue and red regions indicate positive (hydrogen-bond donors) and negative (hydrogen-bond acceptors) electrostatic potentials.

The overall two-dimensional fingerprint plot is shown in Fig. 6*a* and those delineated into H···H, H···Cl/Cl···H, H···S/S···H, H···C/C ··· H, C···Cl/Cl···C, Cl···Cl, N···Cl/Cl···N, H···N/N···H, C···C and S···Cl/Cl···S interactions are illustrated in Fig. 6(*b*)–(*k*), respectively. According to the two-dimensional fingerprint plots the H···H, H···Cl/Cl···H, and H···S/S···H contacts make the most significant contri-

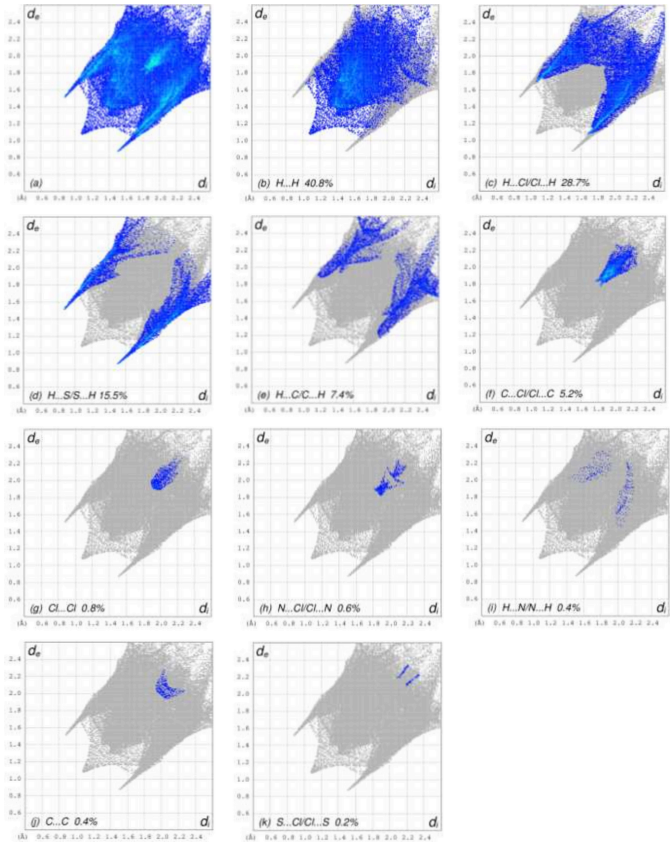

Figure 6
The two-dimensional fingerprint plots for title molecule, showing (*a*) all interactions, and delineated into (*b*) H···H, (*c*) H···Cl/Cl···H, (*d*) H···S/S···H, (*e*) H···C/C···H, (*f*) C···Cl/Cl···C, (*g*) Cl···Cl, (*h*) N···Cl/Cl···N, (i) H···N/N···H, (*j*) C···C and (*k*) S···Cl/Cl···S interactions. The d_i and d_e values are the closest internal and external distances (in Å) from given points on the Hirshfeld surface.

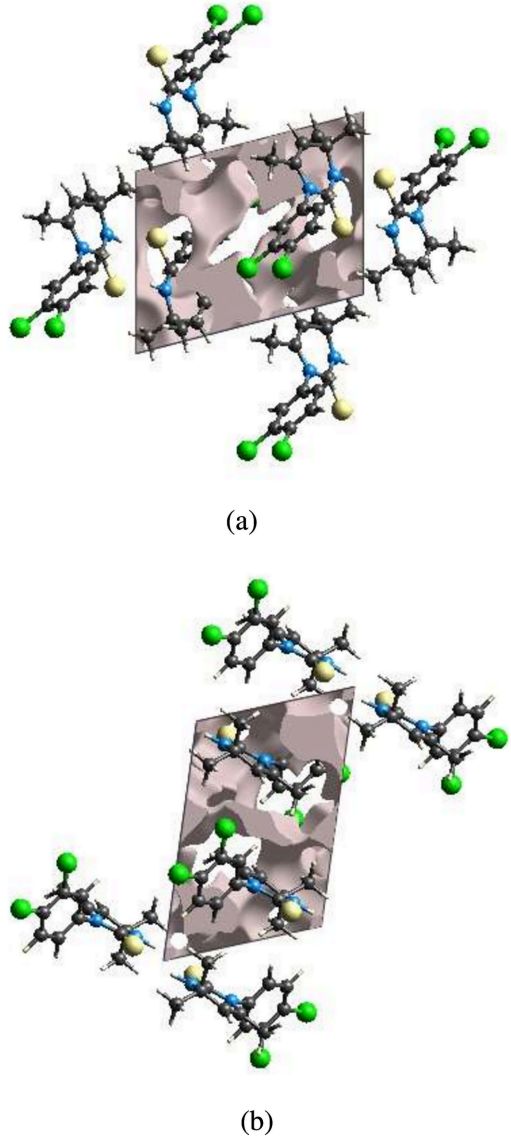

Figure 7
Crystal voids viewed down the (*a*) *a*-axis and (*b*) *b*-axis directions.

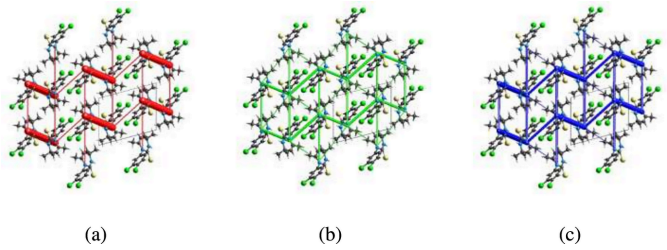

Figure 8
The energy frameworks for a cluster of molecules of the title compound viewed down the *a*-axis showing the (*a*) electrostatic energy, (*b*) dispersion energy and (*c*) total energy diagrams. The cylindrical radius is proportional to the relative strength of the corresponding energies and they were adjusted to the same scale factor of 80 with cut-off value of 5 kJ mol^{-1} within 2 × 2 × 2 unit cells.

butions to the HS, at 40.8%, 28.7% and 15.5%, respectively (Fig. 6).

The strength of the crystal packing depends on the tight packing of the molecules, which results in insignificant voids. To check the strength of the crystal, a void analysis was performed. The volume of the crystal voids (Fig. 7*a* and *b*) and the percentage of free space in the unit cell were calculated to be 135.01 Å^3 and 17.99%, respectively. Thus, the crystal packing appears to be not compact.

The intermolecular interaction energies are calculated using the CE–B3LYP/6–31G(d,p) energy model available in *CrystalExplorer* 17.5 (Spackman *et al.*, 2021), where a cluster of molecules is generated by applying crystallographic symmetry operations with respect to a selected central molecule within the radius of 3.8 Å by default. The total intermolecular energy (E_{tot}) is the sum of electrostatic (E_{ele}), polarization (E_{pol}), dispersion (E_{dis}) and exchange-repulsion (E_{rep}) energies (Turner *et al.*, 2015) with scale factors of 1.057, 0.740, 0.871 and 0.618, respectively (Mackenzie *et al.*, 2017). Hydrogen-bonding interaction energies (in kJ mol^{-1}) were calculated to be −80.2 (E_{ele}), −20.0 (E_{pol}), −22.8 (E_{dis}), 70.4 (E_{rep}) and −58.2 (E_{tot}) for N2—H2*N*···S1.

Energy frameworks combine the calculation of intermolecular interaction energies with a graphical representation of their magnitudes, in which they were constructed for E_{ele} (red cylinders), E_{dis} (green cylinders) and E_{tot} (blue cylinders) (Fig. 8*a*, *b* and *c*). The evaluations of the electrostatic, dispersion and total energy frameworks indicate that the stabilization is dominated *via* the electrostatic energy contributions in the crystal structure of the title compound.

4. Database survey

A search of the Cambridge Structural Database (CSD, Version 6.00, updated May 2025; Groom *et al.*, 2016) revealed six closely related structures of 1-aryl-4,4,6-trimethyl-3,4-dihydropyrimidine-2(1*H*)-thione derivative, *viz.*: 1-(4-fluorophenyl)-4,4,6-trimethyl-3,4-dihydropyrimidine-2(1*H*)-thione, $C_{13}H_{15}FN_2S$ (CSD refcode ASEHIR; Kadir *et al.*, 2016), 1-(3-chlorophenyl)-4,4,6-trimethyl-3,4-dihydropyrimidine-2(1*H*)-thione, $C_{13}H_{15}ClN_2S$ (CSD refcode IJUGEA; Yamin & Salem, 2011*a*), 1-(3-fluorophenyl)-4,4,6-trimethyl-3,4-dihydropyrimidine-2(1*H*)-thione, $C_{13}H_{15}FN_2S$ (CSD refcode EVEWIM; Yamin *et al.*, 2011*b*), 4,4,6-trimethyl-1-phenyl-3,4-dihydropyrimidine-2(1*H*)-thione, $C_{13}H_{16}N_2S$ (Yamin *et al.*, 2005), 1-(4-chlorophenyl)-4,4,6-trimethyl-3,4-dihydropyrimidine-2(1*H*)-thione, $C_{13}H_{15}ClN_2S$ (CSD refcode DUNZIW; Saeed & Bolte, 2010*a*) and 4,4,6-trimethyl-1-(3-methylphenyl)-3,4-dihydropyrimidine-2(1*H*)-thione, $C_{14}H_{18}N_2S$ (CSD refcode PUJYID; Saeed *et al.*, 2010*b*). The title compound differs from these reported structures by the presence of chlorine substituents at both the 3- and 4- positions of the phenyl ring. Similar to several related derivatives, the crystal packing is consolidated by N—H···S hydrogen bonds, forming centrosymmetric dimers.

Table 2
Experimental details.

Crystal data	
Chemical formula	$C_{13}H_{14}Cl_2N_2S$
M_r	301.22
Crystal system, space group	Triclinic, $P\overline{1}$
Temperature (K)	293
a, *b*, *c* (Å)	7.916 (1), 8.927 (1), 11.759 (2)
α, β, γ (°)	99.93 (1), 107.18 (1), 102.32 (1)
V (Å^3)	750.52 (19)
Z	2
Radiation type	Mo *K*α
μ (mm^{-1})	0.56
Crystal size (mm)	0.50 × 0.36 × 0.34
Data collection	
Diffractometer	Oxford Diffraction Xcalibur with Sapphire CCD
Absorption correction	Multi-scan (*CrysAlis RED*; Oxford Diffraction, 2006
T_{min}, T_{max}	0.769, 0.834
No. of measured, independent and observed [$I > 2\sigma(I)$] reflections	5185, 3026, 2502
R_{int}	0.014
(sin $\theta/\lambda)_{max}$ (Å^{-1})	0.625
Refinement	
$R[F^2 > 2\sigma(F^2)]$, $wR(F^2)$, *S*	0.047, 0.131, 1.09
No. of reflections	3026
No. of parameters	166
No. of restraints	1
H-atom treatment	H atoms treated by a mixture of independent and constrained refinement
$\Delta\rho_{max}$, $\Delta\rho_{min}$ (e Å^{-3})	0.34, −0.36

Computer programs: *CrysAlis CCD* and *CrysAlis RED* (Oxford Diffraction, 2006), *SHELXT2014/5* (Sheldrick, 2015*a*), *SHELXL2018/3* (Sheldrick, 2015*b*), *ORTEP-3 for Windows* and *WinGX* publication routines (Farrugia, 2012) and *PLATON* (Spek, 2020).

5. Synthesis and crystallization

3,4-Dichloro aniline (0.16 g, 1.0 mmol) was added portionwise to a stirred solution of potassium thiocyanate (0.09 g, 1.0 mmol) in acetone containing one drop of H_2SO_4 at room temperature. The reaction mixture was then heated at 232–333 K for 3 h while being monitored using thin-layer chromatography. After the reaction was complete, the content was cooled to room temperature, and then poured into ice–water. The resulting precipitate was filtered, dried and recrystallized at room temperature from ethanol solution by gradual

evaporation. Colourless crystals suitable for X-ray analysis were obtained by slow evaporation of acetonitrile. Colourless, yield 86%, m.p. 468 K, IR (KBr) cm^{-1}: 3285 (N—H str.), 1530 (C═S str.), 3176 (Ar. C—H str.).

6. Refinement

Crystal data, data collection and structure refinement details are summarized in Table 2. The NH hydrogen atoms were located from difference-Fourier maps and refined isotropically. The C-bound hydrogen-atom positions were calculated geometrically at distances of 0.93 Å (for aromatic CH) and 0.96 Å (for methyl CH) and refined using a riding model by applying the constraint $U_{iso}(H) = k \times U_{eq}$ (C), where $k = 1.5$ for methyl hydrogens and $k = 1.2$ for the other H atoms.

Acknowledgements

The authors thank the Yenepoya Deemed to be University for the facilities and financial support. TH is also grateful to Hacettepe University Scientific Research Project Unit (grant No. 013 D04 602 004). The authors' contributions are as follows. Conceptualization, SK and TH; synthesis, SK; X-ray analysis, SK and TH; Hirshfeld surface analysis, TH; writing (review and editing of the manuscript) SK and TH; supervision, TH and SK.

References

Alam, O., Imran, M. & Khan, S. A. (2005). *Indian J. Heterocycl. Chem.* **14**, 293–296.
Allen, F. H., Kennard, O., Watson, D. G., Brammer, L., Orpen, A. G. & Taylor, R. (1987). *J. Chem. Soc. Perkin Trans. 2* pp. S1–19.
Cremer, D. & Pople, J. A. (1975). *J. Am. Chem. Soc.* **97**, 1354–1358.
Etter, M. C., MacDonald, J. C. & Bernstein, J. (1990). *Acta Cryst.* B**46**, 256–262.
Farrugia, L. J. (2012). *J. Appl. Cryst.* **45**, 849–854.
Groom, C. R., Bruno, I. J., Lightfoot, M. P. & Ward, S. C. (2016). *Acta Cryst.* B**72**, 171–179.
Kadir, A., Abd Malek, N. A., Mohd Zaki, H., Hasbullah, S. A. & Yamin, B. M. (2016). *IUCrData* **1**, x161189.
Kappe, C. O. (2000). *Acc. Chem. Res.* **33**, 879–888.
Leite, A. C. L., de Lima, R. S., Moreira, D. R. M., Cardoso, M. V. O., Gouveia de Brito, A. C., Farias dos Santos, L. M., Hernandes, M. Z., Kiperstok, A. C., de Lima, R. S. & Soares, M. B. P. (2006). *Bioorg. Med. Chem.* **14**, 3749–3757.
Mackenzie, C. F., Spackman, P. R., Jayatilaka, D. & Spackman, M. A. (2017). *IUCrJ* **4**, 575–587.
Oxford Diffraction (2006). *CrysAlis CCD* and *CrysAlis RED* Oxford Diffraction Ltd, Abingdon, England.
Özçelik, S., Dinçer, M., Yıldırım, İ. & Akçamur, Y. (2004). *Acta Cryst.* E**60**, o1123–o1125.
Saeed, A. & Bolte, M. (2010*a*). *Acta Cryst.* E**66**, o440.
Saeed, A., Khera, R. A. & Parvez, M. (2010*b*). *Acta Cryst.* E**66**, o635.
Sheldrick, G. M. (2015*a*). *Acta Cryst.* A**71**, 3–8.
Sheldrick, G. M. (2015*b*). *Acta Cryst.* C**71**, 3–8.
Spackman, P. R., Turner, M. J., McKinnon, J. J., Wolff, S. K., Grimwood, D. J., Jayatilaka, D. & Spackman, M. A. (2021). *J. Appl. Cryst.* **54**, 1006–1011.
Spek, A. L. (2020). *Acta Cryst.* E**76**, 1–11.
Sriram, D., Yogeeswari, P. & Devakaram, R. V. (2006). *Bioorg. Med. Chem.* **14**, 3113–3118.
Turner, M. J., Thomas, S. P., Shi, M. W., Jayatilaka, D. & Spackman, M. A. (2015). *Chem. Commun.* **51**, 3735–3738.
Yamin, B. M., Kasim, N. A. M. & Hamzah, N. (2005). *Acta Cryst.* E**61**, o55–o57.
Yamin, B. M., Lawi, R. L. & Salem, H. F. (2011*b*). *Acta Cryst.* E**67**, o1810.
Yamin, B. M. & Salem, H. F. (2011*a*). *Acta Cryst.* E**67**, o282.
Yamin, B. M. & Yusof, M. S. M. (2003). *Acta Cryst.* E**59**, o151–o152.

supporting information

Acta Cryst. (2026). E**82**, 937-941 [https://doi.org/10.1107/S2056989026007231]

Synthesis, crystal structure and Hirshfeld surface analysis of 1-(3,4-dichlorophenyl)-4,4,6-trimethyl-3,4-dihydropyrimidine-2(1*H*)-thione

Sharatha Kumar and Tuncer Hökelek

Computing details

1-(3,4-Dichlorophenyl)-4,4,6-trimethyl-3,4-dihydropyrimidine-2(1*H*)-thione

Crystal data

$C_{13}H_{14}Cl_2N_2S$
$M_r = 301.22$
Triclinic, $P\overline{1}$
$a = 7.916$ (1) Å
$b = 8.927$ (1) Å
$c = 11.759$ (2) Å
$\alpha = 99.93$ (1)°
$\beta = 107.18$ (1)°
$\gamma = 102.32$ (1)°
$V = 750.52$ (19) Å^3
$Z = 2$
$F(000) = 312$
$D_x = 1.333$ Mg m^{-3}
Mo $K\alpha$ radiation, $\lambda = 0.71073$ Å
Cell parameters from 2526 reflections
$\theta = 2.7$–27.9°
$\mu = 0.56$ mm^{-1}
$T = 293$ K
Prism, colourless
0.50 × 0.36 × 0.34 mm

Data collection

Oxford Diffraction Xcalibur with Sapphire CCD diffractometer
Rotation method data acquisition using ω scans.
Absorption correction: multi-scan (CrysAlis RED; Oxford Diffraction, 2006
$T_{min} = 0.769$, $T_{max} = 0.834$
5185 measured reflections
3026 independent reflections
2502 reflections with $I > 2\sigma(I)$
$R_{int} = 0.014$
$\theta_{max} = 26.4$°, $\theta_{min} = 2.7$°
$h = -9 \rightarrow 9$
$k = -10 \rightarrow 11$
$l = -14 \rightarrow 14$

Refinement

Refinement on F^2
Least-squares matrix: full
$R[F^2 > 2\sigma(F^2)] = 0.047$
$wR(F^2) = 0.131$
$S = 1.09$
3026 reflections
166 parameters
1 restraint
Hydrogen site location: mixed
H atoms treated by a mixture of independent and constrained refinement
$w = 1/[\sigma^2(F_o^2) + (0.0531P)^2 + 0.5196P]$ where $P = (F_o^2 + 2F_c^2)/3$
$(\Delta/\sigma)_{max} < 0.001$
$\Delta\rho_{max} = 0.34$ e Å^{-3}
$\Delta\rho_{min} = -0.36$ e Å^{-3}

Special details

Geometry. All esds (except the esd in the dihedral angle between two l.s. planes) are estimated using the full covariance matrix. The cell esds are taken into account individually in the estimation of esds in distances, angles and torsion angles; correlations between esds in cell parameters are only used when they are defined by crystal symmetry. An approximate (isotropic) treatment of cell esds is used for estimating esds involving l.s. planes.

Fractional atomic coordinates and isotropic or equivalent isotropic displacement parameters (Å²)

	x	*y*	*z*	U_{iso}*/U_{eq}
C1	0.3026 (3)	0.5937 (3)	0.1548 (2)	0.0422 (5)
C2	0.2695 (4)	0.8680 (3)	0.1621 (3)	0.0603 (7)
C3	0.4444 (5)	0.9152 (4)	0.2678 (4)	0.0816 (11)
H3	0.485846	1.019411	0.314955	0.098*
C4	0.5456 (4)	0.8184 (3)	0.2995 (3)	0.0627 (8)
C5	0.5946 (3)	0.5528 (3)	0.2628 (2)	0.0434 (5)
C6	0.5958 (3)	0.4814 (3)	0.3573 (2)	0.0465 (6)
H6	0.516423	0.494028	0.400471	0.056*
C7	0.7150 (4)	0.3909 (3)	0.3879 (2)	0.0480 (6)
C8	0.8296 (4)	0.3696 (3)	0.3222 (3)	0.0540 (6)
C9	0.8260 (4)	0.4402 (4)	0.2263 (3)	0.0649 (8)
H9	0.902697	0.425268	0.181383	0.078*
C10	0.7088 (4)	0.5327 (4)	0.1971 (3)	0.0574 (7)
H10	0.707063	0.581304	0.133010	0.069*
C11	0.2915 (7)	0.9217 (5)	0.0513 (4)	0.1110 (16)
H11A	0.333986	1.035250	0.071888	0.166*
H11B	0.379489	0.878031	0.026262	0.166*
H11C	0.174966	0.885896	−0.014726	0.166*
C12	0.1231 (6)	0.9308 (5)	0.1992 (5)	0.1088 (15)
H12A	0.162291	1.044564	0.221850	0.163*
H12B	0.008837	0.894392	0.131086	0.163*
H12C	0.106251	0.892958	0.267781	0.163*
C13	0.7245 (5)	0.8681 (4)	0.4024 (4)	0.0966 (14)
H13A	0.773023	0.778897	0.408496	0.145*
H13B	0.809630	0.949830	0.387448	0.145*
H13C	0.706552	0.907897	0.477922	0.145*
N1	0.4778 (3)	0.6555 (2)	0.23637 (19)	0.0465 (5)
N2	0.2043 (3)	0.6938 (3)	0.1281 (2)	0.0554 (6)
Cl1	0.71964 (14)	0.30829 (10)	0.51126 (7)	0.0761 (3)
Cl2	0.98030 (13)	0.25664 (12)	0.35758 (10)	0.0907 (3)
S1	0.21347 (9)	0.39621 (7)	0.09242 (7)	0.0518 (2)
H2N	0.094 (3)	0.652 (3)	0.078 (2)	0.062*

Atomic displacement parameters (Å²)

	U^{11}	U^{22}	U^{33}	U^{12}	U^{13}	U^{23}
C1	0.0414 (12)	0.0430 (12)	0.0441 (12)	0.0150 (10)	0.0137 (10)	0.0139 (10)
C2	0.0642 (17)	0.0437 (14)	0.0679 (18)	0.0224 (13)	0.0089 (14)	0.0166 (13)
C3	0.079 (2)	0.0437 (16)	0.095 (3)	0.0202 (15)	−0.0047 (19)	0.0087 (16)

C4	0.0581 (16)	0.0415 (14)	0.0708 (19)	0.0116 (12)	0.0006 (14)	0.0107 (13)
C5	0.0388 (12)	0.0433 (12)	0.0455 (13)	0.0140 (10)	0.0106 (10)	0.0082 (10)
C6	0.0527 (14)	0.0453 (13)	0.0455 (13)	0.0204 (11)	0.0185 (11)	0.0102 (10)
C7	0.0562 (15)	0.0394 (12)	0.0436 (13)	0.0176 (11)	0.0097 (11)	0.0068 (10)
C8	0.0468 (14)	0.0476 (14)	0.0623 (16)	0.0227 (11)	0.0094 (12)	0.0052 (12)
C9	0.0557 (17)	0.078 (2)	0.0727 (19)	0.0291 (15)	0.0333 (15)	0.0167 (16)
C10	0.0533 (15)	0.0718 (18)	0.0558 (16)	0.0226 (13)	0.0234 (13)	0.0240 (14)
C11	0.144 (4)	0.072 (2)	0.103 (3)	0.007 (3)	0.028 (3)	0.042 (2)
C12	0.090 (3)	0.083 (3)	0.138 (4)	0.046 (2)	0.020 (3)	−0.007 (3)
C13	0.075 (2)	0.0499 (17)	0.118 (3)	0.0162 (16)	−0.022 (2)	0.0000 (18)
N1	0.0443 (11)	0.0431 (11)	0.0505 (12)	0.0162 (9)	0.0104 (9)	0.0134 (9)
N2	0.0468 (12)	0.0428 (12)	0.0681 (15)	0.0166 (10)	0.0048 (11)	0.0137 (10)
Cl1	0.1138 (7)	0.0656 (5)	0.0650 (5)	0.0473 (5)	0.0301 (5)	0.0312 (4)
Cl2	0.0794 (6)	0.0843 (6)	0.1211 (8)	0.0566 (5)	0.0286 (5)	0.0269 (5)
S1	0.0471 (4)	0.0416 (3)	0.0619 (4)	0.0150 (3)	0.0103 (3)	0.0129 (3)

Geometric parameters (Å, º)

C1—N2	1.323 (3)	C7—Cl1	1.732 (3)
C1—N1	1.361 (3)	C8—C9	1.379 (4)
C1—S1	1.692 (2)	C8—Cl2	1.726 (3)
C2—N2	1.472 (3)	C9—C10	1.378 (4)
C2—C3	1.480 (4)	C9—H9	0.9300
C2—C11	1.507 (5)	C10—H10	0.9300
C2—C12	1.529 (5)	C11—H11A	0.9600
C3—C4	1.326 (4)	C11—H11B	0.9600
C3—H3	0.9300	C11—H11C	0.9600
C4—N1	1.419 (3)	C12—H12A	0.9600
C4—C13	1.484 (4)	C12—H12B	0.9600
C5—C6	1.371 (3)	C12—H12C	0.9600
C5—C10	1.372 (4)	C13—H13A	0.9600
C5—N1	1.443 (3)	C13—H13B	0.9600
C6—C7	1.378 (3)	C13—H13C	0.9600
C6—H6	0.9300	N2—H2N	0.851 (17)
C7—C8	1.376 (4)		
N2—C1—N1	117.4 (2)	C8—C9—H9	120.0
N2—C1—S1	121.53 (19)	C5—C10—C9	119.7 (3)
N1—C1—S1	121.06 (17)	C5—C10—H10	120.1
N2—C2—C3	107.2 (2)	C9—C10—H10	120.1
N2—C2—C11	108.3 (3)	C2—C11—H11A	109.5
C3—C2—C11	113.0 (3)	C2—C11—H11B	109.5
N2—C2—C12	107.8 (3)	H11A—C11—H11B	109.5
C3—C2—C12	110.5 (3)	C2—C11—H11C	109.5
C11—C2—C12	109.8 (3)	H11A—C11—H11C	109.5
C4—C3—C2	124.2 (3)	H11B—C11—H11C	109.5
C4—C3—H3	117.9	C2—C12—H12A	109.5
C2—C3—H3	117.9	C2—C12—H12B	109.5

C3—C4—N1	119.2 (3)	H12A—C12—H12B	109.5
C3—C4—C13	123.9 (3)	C2—C12—H12C	109.5
N1—C4—C13	116.9 (2)	H12A—C12—H12C	109.5
C6—C5—C10	120.6 (2)	H12B—C12—H12C	109.5
C6—C5—N1	119.4 (2)	C4—C13—H13A	109.5
C10—C5—N1	119.9 (2)	C4—C13—H13B	109.5
C5—C6—C7	119.8 (2)	H13A—C13—H13B	109.5
C5—C6—H6	120.1	C4—C13—H13C	109.5
C7—C6—H6	120.1	H13A—C13—H13C	109.5
C8—C7—C6	120.0 (2)	H13B—C13—H13C	109.5
C8—C7—Cl1	121.2 (2)	C1—N1—C4	121.1 (2)
C6—C7—Cl1	118.7 (2)	C1—N1—C5	119.6 (2)
C7—C8—C9	119.9 (2)	C4—N1—C5	119.2 (2)
C7—C8—Cl2	121.4 (2)	C1—N2—C2	127.5 (2)
C9—C8—Cl2	118.8 (2)	C1—N2—H2N	116 (2)
C10—C9—C8	120.0 (3)	C2—N2—H2N	116 (2)
C10—C9—H9	120.0		

N2—C2—C3—C4	17.7 (5)	N2—C1—N1—C4	6.2 (4)
C11—C2—C3—C4	−101.6 (5)	S1—C1—N1—C4	−172.6 (2)
C12—C2—C3—C4	134.9 (4)	N2—C1—N1—C5	−176.2 (2)
C2—C3—C4—N1	−5.7 (6)	S1—C1—N1—C5	5.0 (3)
C2—C3—C4—C13	177.4 (4)	C3—C4—N1—C1	−8.0 (5)
C10—C5—C6—C7	1.2 (4)	C13—C4—N1—C1	169.1 (3)
N1—C5—C6—C7	−176.1 (2)	C3—C4—N1—C5	174.3 (3)
C5—C6—C7—C8	−1.4 (4)	C13—C4—N1—C5	−8.6 (4)
C5—C6—C7—Cl1	177.59 (19)	C6—C5—N1—C1	−90.2 (3)
C6—C7—C8—C9	0.5 (4)	C10—C5—N1—C1	92.5 (3)
Cl1—C7—C8—C9	−178.4 (2)	C6—C5—N1—C4	87.5 (3)
C6—C7—C8—Cl2	−179.8 (2)	C10—C5—N1—C4	−89.7 (3)
Cl1—C7—C8—Cl2	1.3 (3)	N1—C1—N2—C2	9.7 (4)
C7—C8—C9—C10	0.5 (4)	S1—C1—N2—C2	−171.5 (2)
Cl2—C8—C9—C10	−179.2 (2)	C3—C2—N2—C1	−20.4 (4)
C6—C5—C10—C9	−0.1 (4)	C11—C2—N2—C1	101.9 (4)
N1—C5—C10—C9	177.1 (3)	C12—C2—N2—C1	−139.4 (3)
C8—C9—C10—C5	−0.7 (5)		

Hydrogen-bond geometry (Å, º)

D—H···*A*	*D*—H	H···*A*	*D*···*A*	*D*—H···*A*
N2—H2*N*···S1^{i}	0.85 (2)	2.55 (2)	3.375 (2)	163 (3)

Symmetry code: (i) −*x*, −*y*+1, −*z*.